Detecting ultrasonic signals in a turbulent atmosphere: performance of different codes

Fernando J. Álvarez, Jesús Ureña*, Álvaro Hernández*, Ana Jiménez*
Carlos de Marziani*, José M. Villadangos*, M. Carmen Pérez*

Dept. of Electrical Eng., Electronics and Automatics, University of Extremadura, SPAIN
*Dept. of Electronics, University of Alcalá, SPAIN
fernando@depeca.uah.es

Abstract – **Signal coding and pulse compression provide ultrasonic systems with the capability to obtain accurate measurements that are nearly independent of the conditions of operation. This property, together with the high robustness to noise also achived with these techniques, are making possible the development of high reliability systems intended for outdoor operation. However, these systems must face new problems not found indoors, such as the effect of atmospheric turbulence on the shape of the emitted waveforms. This work presents a comparative analysis of the performance of different codes that are used to encode the signals of an ultrasonic sensory system designed to operate under strong turbulence conditions.**

Keywords – **Ultrasonic sensory systems, pulse compression, atmospheric turbulence**

I. INTRODUCTION

High-precision applications of airborne ultrasonic sensory systems have been usually restricted to indoor environments. There are only few works that propose the use of ultrasonic sensors outdoors, and these sensors are, almost always, part of a more complex sensory system where they have been assigned low-precision tasks [1][2]. The low confidence in the results provided by ultrasonic sensors outdoors is mainly due to the large influence that meteorological phenomena have on the propagation of these mechanical waves. Changes in temperature and humidity, the presence of fog or dust in the atmosphere and wind-induced refraction can cause strong variations in the attenuation of acoustic waves [3][4]. Clearly, the measurements provided by a classical system, based on threshold detection of the signal envelope, are extremely sensitive to the conditions of operation.

This problem can be overcome by encoding the signal and introducing pulse compression techniques that have been already used with success in the design of high-performance indoor sonars [5][6][7]. However, a new problem arises in this case. It is well known from outdoor acoustics that atmospheric turbulence causes random fluctuations in the amplitude and the phase of traveling sound waves [8]. Depending on how much the shape of the transmitted signals is modified by this effect, they could not be properly recovered by matched filtering.

In a recent paper, the authors have demonstrated that ultrasonic encoded signals can be detected in a turbulent atmosphere whenever the duration of the emission is below the coherence time of this atmosphere [9]. This result was obtained by means of a new sonar prototype that performs the emission of complementary sets of sequences with BPSK modulation. In the same work, it was also experimentally proved that, when the duration of the emission is above the coherence time, two undesirable effects arise: the appearance of spurious peaks in the correlation process and the deviation of the actual peaks with respect to their expected positions. However, these effects were observed only with the emission of complementary sets, and no other codes were analysed. Complementary sets of sequences constitute a family of binary codes with ideal correlation properties [10], and they are characterized by a high level of symmetry that can be especially sensitive to the effect of turbulence.

The main objective of this paper is to carry out a comparative analysis to verify whether the above mentioned effects are also observed when other codes are emitted, and if so, to evaluate their magnitude in relation to the ratio between the emission time and the coherence time.

The rest of the paper is organized as follows: Section II presents the semi-empiric model for a turbulent atmosphere used to conduct the comparative analysis. In Section III the performance of differentd codes is analyzed in terms of two parameters: the Mainlobe-to-Sidelobe Ration and the shift of the autocorrelation peak. Section IV investigates the effect of turbulence on the orthogonality of a family of codes, and

1-4244-0830-X/07/$20.00 ©2007 IEEE.

finally, the main conclusions of these work are outlined in Section V.

II. Model for a Turbulent Atmosphere

When wind blows in the lower layers of the atmosphere it rarely does in a stationary way and almost always random fluctuations of its behaviour appear in the form of highly rotational fluxes. These *turbulent eddies* cause local random fluctuations in wind velocity and temperature, two parameters which have strong influence on the propagation velocity of acoustic waves. When an acoustic wave propagates through a turbulent region, it encounters a variety of eddies with different sizes, velocities and temperatures. Each one of these eddies acts as a strong scatterer of acoustic energy and their combined effect alters the initial coherence of the wavefronts, which will no longer be spherical and with identical amplitude after crossing the turbulent region. This situation is depicted in Fig. 1. A receiver placed at a certain distance from the emitter will record random fluctuations in the amplitude and phase of the acquired signals.

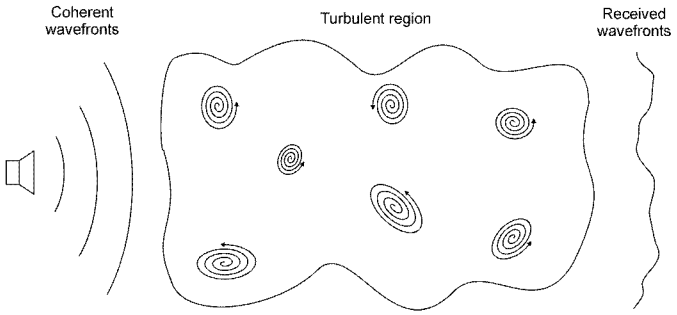

Fig. 1. Propagation of an acoustic wave through a turbulent medium..

These effects can be characterized through the coherence time t_c, defined as the time during which the characteristics of an acoustic wave propagating through a turbulent region remain essentially invariant. Assuming a frozen model for the turbulent atmosphere [11], the coherence time is given by:

$$t_c = \frac{1}{v_n \cdot \left(0.545 k^2 C_n^2 r\right)^{3/5}} \qquad (1)$$

where v_n is the transversal component of the wind; k is the wavenumber; r is the propagation distance; and C_n^2 is the structure parameter of the refractive index, which is a measure of the turbulence strength.

With the aim of gaining a better understanding of the effects that atmospheric turbulence has on the propagation of ultrasonic signals, an exhaustive analysis of the amplitude and phase fluctuations undergone by a 50 kHz tone continuously emitted under different turbulence conditions have been performed. This analysis has been carried out by splitting the received signal in segments of 16 samples, corresponding to one cycle of a 50 kHz tone sampled at a rate of 800 kHz. Amplitude fluctuations were studied by calculating the energy of the samples contained in every segment. To analyze phase fluctuations, a set of 16 pattern vectors were generated corresponding to the 16 identifiable phases obtained when sampling a 50 kHz tone at a rate of 800 kHz ($-\pi + k \cdot \pi/8$ with k = 0, … ,15). The phase of the segment under analysis was chosen as the phase of the pattern vector whose Euclidean distance to this segment is minimum. Figure 2 shows the amplitude and phase fluctuations registered outdoors under very strong turbulence conditions for one second.

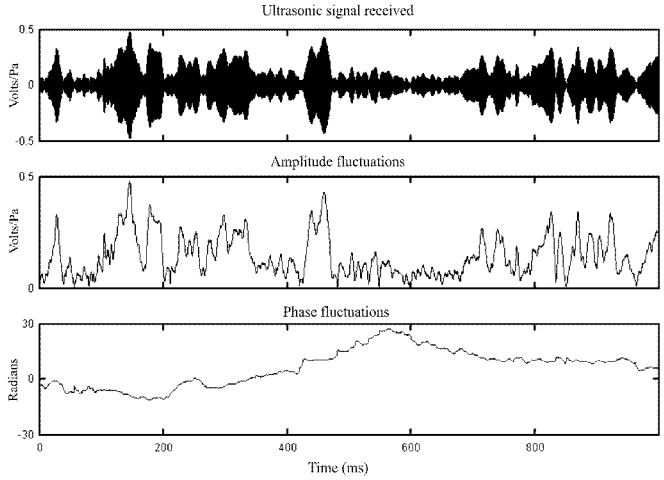

Fig. 2. Amplitude and phase fluctuations observed outdoors for a 50 kHz ultrasonic tone continuously emitted under very strong turbulence conditions.

After analyzing a total of 200 emissions, 2 seconds long each, it has been observed that, under strong and very strong turbulence conditions, phase ϕ fluctuations fit well to a uniform distribution, whereas amplitude A fluctuations do the same to a Weibull distribution as follows:

$$p(A) = \left(\frac{\beta}{A}\right) \cdot \left(\frac{A}{\eta}\right)^{\beta} \cdot \exp\left[-\left(\frac{A}{\eta}\right)^{\beta}\right] \qquad (2)$$

where β and η are the shape and scale parameters of this distribution respectively. Values of β in the interval [1.3 - 3.1] have been measured, although this value is typically around 1.6. The scale parameter η is directly related to the expected amplitude in absence of turbulence A_0 as $\eta \approx A_0/2$. Under these strong turbulence conditions, the coherence time acquires a clear physical meaning as the time for which the rates of change of the amplitude and the phase are essentially constant.

All these results have led to the proposal of a semi-empiric model for a turbulent atmosphere as a dynamic channel where an ultrasonic tone can undergone, after a coherence time, any phase change between $-\pi$ and π radians with identical probability. Also, after this time the amplitude can take any positive value with a probability given by a Weibull

distribution characterized by $\beta = 1.6$ and $\eta = A_0/2$. The model assumes that during a coherence time, both the amplitude and the phase vary linearly between two random values. Figure 3 shows the amplitude and phase fluctuations predicted by this model for a coherence time of 10 ms (very strong turbulence conditions).

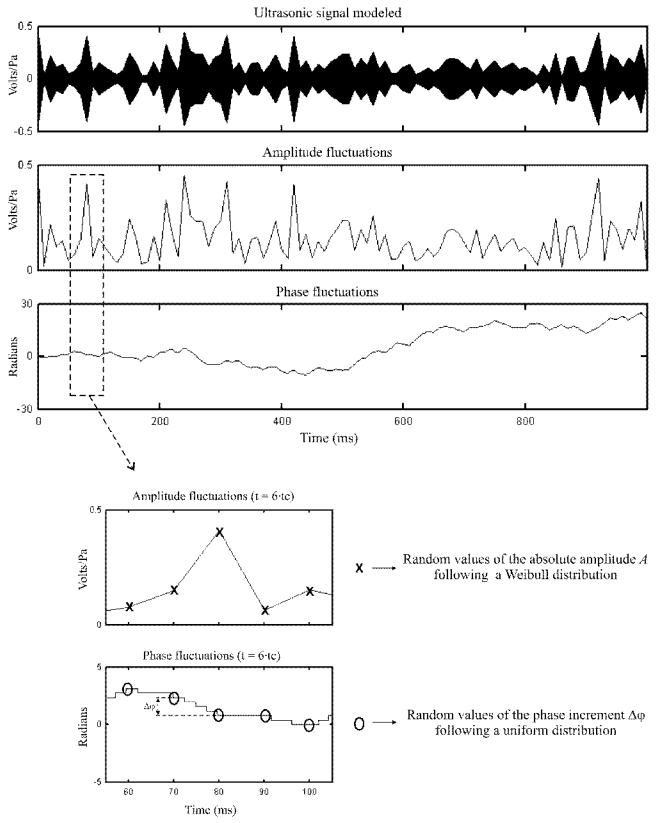

Fig. 3. Amplitude and phase fluctuations predicted by the model for a 50 kHz ultrasonic tone and a coherence time of 10 ms

The model for pure tones can be easily adapted to signals with a narrow bandwidth around the carrier frequency. In this case, the model assumes that the ratio between the real amplitude and the expected one follows the same Weibull distribution. Besides, after a coherence time the signal can undergone with identical probability any compression or expansion between zero and one half the carrier cycle. This is equivalent to assume that, as in the model for a pure tone, the carrier can undergone any phase change between $-\pi$ and π with identical probability, whereas the rest of the spectral components experience a phase shift proportional to their frequency. Note that this model is only valid for narrow band signals, since it does not consider the dependence on frequency of the coherence time predicted by (1).

III. PERFORMANCE OF DIFFERENT CODES

The model presented in the previous section has been used to investigate the effect of a turbulent atmosphere on the detection of ultrasonic encoded signals by matched filtering. Particularly, three different codes with similar lengths have been analyzed: an extended Barker code of 11 × 11 =121 bits, a Gold sequence of 127 bits, and a Golay pair of 2 × 64 bits. All these codes are BPSK modulated with a symbol of two cycles of a 50 kHz carrier, thus obtaining the emission patterns that are filtered to simulate the transduction effect of the well-known Polaroid electrostatic transducer [12]. The turbulence model is then applied to the filtered signals to obtain the received waves, which are correlated with the original patterns to simulate the detection process. Two features of these autocorrelation signals have been measured:

1. Sidelobe-to-Mainlobe Ratio (*SMR*): defined as the ratio between the maximum value measured outside the main lobe, to the maximum value obtained inside this lobe. The width of the main lobe depends on the modulation symbol, and it is 75 μs long in our case. The *SMR* is a measure of the ease with which the codes can be detected by matched filtering.

2. Shift of the autocorrelation peak: defined as the distance between the position of the maximum value obtained in the autocorrelation signal and the expected position of this value. This magnitude represents the error in the estimation of the time of arrival of the signal.

Both magnitudes have been calculated for coherence times t_c equal to 2, 1, 1/2, 1/4 and 1/6 times the emission time of each code t_e, values that represent increasing intensities of turbulence respectively. In the case of the Golay pair, two modes of transmission have been considered: one sequence concatenated just after the other, and both sequences with their bits interleaved. Also, a chirp signal with similar duration than the codes and sweeping linearly from 60 kHz to 40 kHz has been considered in this analysis. The inclusion of this chirp is interesting because this is the type of signal emitted by some species of bats to navigate outdoors.

Table I shows the *SMR* values obtained for the five signals under study and the five ratios tc/te considered. As a reference, the second column in this table shows the *SMR* values for and infinite coherence time, i.e., when no turbulence is considered. The data shown in columns 3 to 7 are actually average values obtained after 500 simulations of each case.

Some comments can be derived from Table I. First, it is surprising to discover that the code with the best performance in absence of turbulence, the extended Barker, is the one with worst *SMR* under intense turbulence. On the contrary, the Gold code, with the second worst *SMR* with an infinite coherence time, presents the second best value under strong turbulence conditions. The performance of the Golay pairs is very similar and, apparently, the mode in which the codes are emitted in not crucial, at least when dealing with this number of bits. No clear conclusion can be drawn for the chirp, as it has the worst *SMR* value in absence of turbulence and presents the second worst one with intense turbulence. These

conclusions are confirmed by Fig.4, where the relative increment of *SMR* with increasing turbulence has been represented. Now, it can be clearly seen that the signal with a lower increment of *SMR* in relative terms is the chirp.

TABLE I.

AVERAGE SIDELOBE-TO-MAINLOBE RATIO

	$t_c = \infty$	$t_c = 2 \cdot t_e$	$t_c = t_e$	$t_c = t_e/2$	$t_c = t_e/4$	$t_c = t_e/6$
Barker	0.0915	0.1281	0.2907	0.5553	0.6944	0.7358
Gold	0.1529	0.1661	0.1972	0.3202	0.4703	0.5356
Golay interl.	0.1502	0.1600	0.1997	0.4178	0.5506	0.6717
Goaly concat.	0.1190	0.1344	0.1716	0.29910	0.4762	0.5753
Chirp	0.2673	0.3813	0.3826	0.4984	0.6765	0.7366

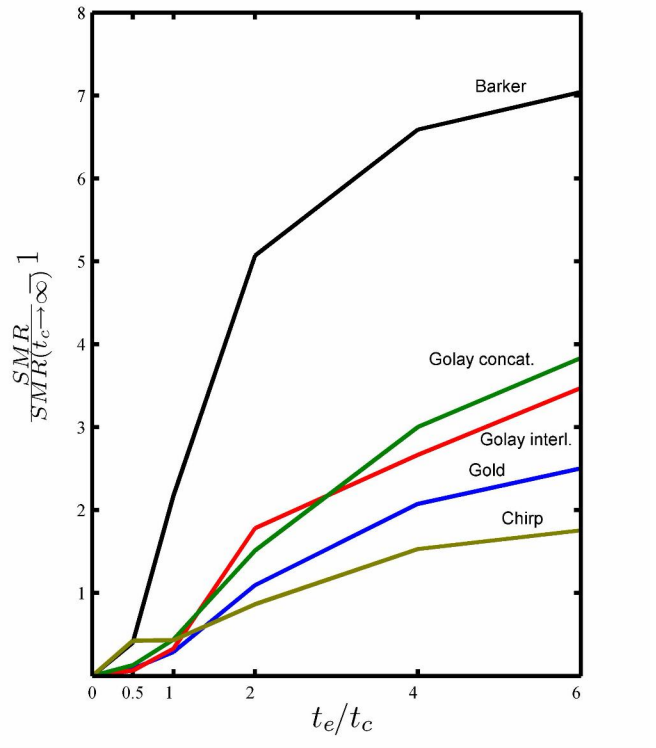

Fig. 4. Relative increment of *SMR* with increasing values of the ratio t_e / t_c.

Regarding the shift of the autocorrelation peak, Table II shows the average value of this shift for all the cases considered before and the same number of simulations −500 per case−. The most important conclusions about the performance of the codes in a turbulent atmosphere can be derived from the analysis of this data.

TABLE II.

AVERAGE SHIFT OF THE AUTOCORRELATION PEAK (μs)

	$t_c = 2 \cdot t_e$	$t_c = t_e$	$t_c = t_e/2$	$t_c = t_e/4$	$t_c = t_e/6$
Barker	1.16	2.17	208.14	578.43	707.35
Gold	1.22	2.09	38.86	84.79	157.49
Golay interl.	1.18	2.07	197.42	642.76	797.45
Goaly concat.	1.20	2.06	44.23	199.46	287.75
Chirp	6.44	10.5	15.16	29.00	45.80

First, it can be clearly seen that when the coherence time is equal or greater than the emission time, the average shift is only of a few μs in all the cases. Moreover, with the sole exception of the chirp, these shifts are always lower than 2.5 μs, that is, one sampling period. This result confirms the main hypothesis of [9] that is in the origin of this work: ultrasonic encoded signal can be reliably detected under turbulent conditions whenever the duration of the emission is below the coherence time of the atmosphere.

When the coherence time starst going below the emission time, the average shift significantly increases. Again, the extended Barker is the code that exhibits the worst performance and the Gold sequence is the best behaved one. Now, a clear different can be seen between the performance of the Golay pairs depending on the method of transmission. The average shift of the autocorrelation peak increases far more rapidly when the sequences are interleaved than when they are concatenated. However, all the codes exhibit an average shift larger than half the main lobe (37.5 μs) when $t_c < t_e$. In this case, the shape of the emitted waveform is being modified so much by turbulence that the autocorrelation peak does not appear (in average) when this signal and its correlation pattern are aligned. The only signal that keeps the value of the average shift inside the analysis window of the main lobe for coherence times as low as $t_e / 4$ is the chirp, that turns out to be the most reliable signal to work with under strong turbulent conditions.

IV. EFFECT OF TURBULENCE ON THE ORTHOGONALITY OF A FAMILY OF CODES

Many ultrasonic sensory systems that encode their signals and detect them by matched filtering can perform the simultaneous emission of some of these signals with the ability to distinguish between them at the receiver. This property can be achieved by selecting a family of binary codes with low values of cross-correlation between them (orthogonal or pseudo-orthogonal codes). The Figure of Merit commonly used to quantify the goodness of performance of a

family with M codes L-bits long each, say $\{ c_i[n]; 0 \le n < L, 0 < i \le M \}$, is the *Bound*, defined as $B = \max(\theta_{AC}, \theta_{CC})$, where θ_{AC} stands for the maximum sidepeak obtained in all the autocorrelations and θ_{CC} is the maximum value obtained in the cross-correlations between all the sequences contained in the family, i.e.:

$$\theta_{AC} = \max\left\{\frac{\phi_{c_i c_i}[k]}{L};\ \forall i \in [1,\ldots,M],\ \forall k \neq 0\right\}$$
$$\theta_{CC} = \max\left\{\frac{\phi_{c_i c_j}[k]}{L};\ \forall i,j \in [1,\ldots,M],\ i \neq j,\ \forall k\right\} \quad (3)$$

where ϕ_{xy}[k] is the aperiodic correlation function of the sequences x and y.

In this section, the model presented before have been used to investigate the effect of a turbulent atmosphere on the Bound of a family with good correlation properties. Three Gold families with different sizes have been selected to conduct this study: a set with 4 codes of 63 bits, another set with 8 codes of 127 bits and a third one with 16 codes of 255 bits. All these codes have been again BSPK modulated to obtain the emission patterns, filtered to obtain the emitted waves, and modified in accordance to the atmosphere model to obtain the received signals. Now, the Bound can be defined in a similar way than before but operating with the modulated patterns p_i and the received signals s_i instead of the codes c_i, and taking into account the number of samples in the modulation symbol N:

$$B = \max(\theta_{AC}, \theta_{CC})$$
$$\theta_{AC} = \max\left\{\frac{\phi_{s_i p_i}[k]}{\max \phi_{s_i p_i}};\ \forall i \in [1,\ldots,M],\ \forall k \notin [-N+1, N-1]\right\}$$
$$\theta_{CC} = \max\left\{\frac{\phi_{s_i p_j}[k]}{\max \phi_{s_i p_j}};\ \forall i,j \in [1,\ldots,M],\ i \neq j,\ \forall k\right\} \quad (4)$$

Table III shows the average Bound of the Gold families for different values of the ratio t_c / t_e. Only values of this ratio equal or greater than 1 are interesting in this analysis, since we already know from the previous section that when $t_c / t < 1$ the received wave is so distorted that the autocorrelation peak does not appear when this signal is aligned with the pattern, and the Bound loses its meaning. However, the last column of this table includes the values of B for $t_c = 0.25 \cdot t_e$ to obtain a new result that should convince anyone to avoid the use of codes with emission times above the coherence time: the cross-correlation between pseudo-orthogonal codes can give higher values than the autocorrelation itself. Second column in this table shows as a reference the Bound for and infinite coherence time, and columns 3 to 7 show again average values obtained after 500 simulations. As expected, the longer the sequences the lower the Bound of the family, although with $t_c = t_e / 4$ the larger families seem to suffer a higher degradation that increases their Bound.

TABLE III.

AVERAGE BOUND OF THREE GOLD FAMILIES WITH DIFFERENT SIZES

	$t_c = \infty$	$t_c = 8 \cdot t_e$	$t_c = 4 \cdot t_e$	$t_c = 2 \cdot t_e$	$t_c = t_e$	$t_c = t_e/4$
4 Codes 63 bits	0.3825	0.3841	0.3975	0.4320	0.5709	1.2566
8 Codes 127 bits	0.2523	0.2607	0.2757	0.3124	0.4655	1.4282
16 Codes 255 bits	0.2129	0.2212	0.2326	0.2452	0.4383	1.5637

Figure 5 shows the relative increment of this Bound when $t_e / t_c \le 1$. It is clear now that to assure an average Bound similar to that measured in absence of turbulence (relative increment less than 10%), the coherence time must be at least 4 times the emission time. For $t_e / t_c \ge 0.5$ the Bound rapidly degrades and, as observed before, this degradation is higher the larger the size of the family is, reaching a value of 105% for a family of 16 codes with 255 bits when $t_e = t_c$.

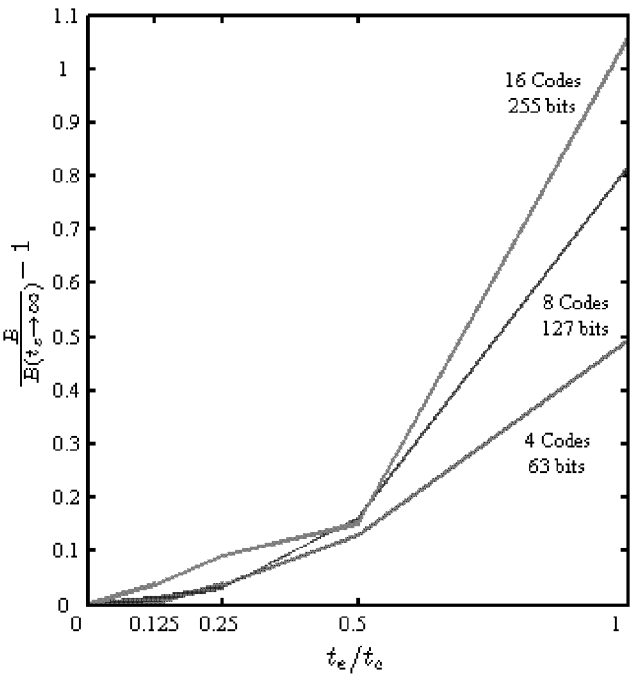

Fig. 5 Relative increment of Bound with increasing values of the ratio t_e / t_c.

V. CONCLUSIONS

This work has presented a comparative analysis of the performance of different codes used in an ultrasonic sensory system that operates outdoors under turbulent conditions. This analysis is based on a semi-empiric model for a turbulent

atmosphere that simulates the effect of this phenomenon on the amplitude and the phase of narrow-band acoustic signals.

It has been shown that all the codes exhibit a good behaviour in terms of Sidelobe-to-Mainlobe ratio and shift of the autocorrelation peak whenever the coherence time of the atmosphere is above the emission time. For coherence times below the emission time the Gold code is the one that presents the best performance among the three types of codes analysed – Barker, Gold and Golay, although the chirp is the only signal that can provide reliable results.

Also the effect of atmospheric turbulence on the correlation properties of a pseudo-orthogonal family of codes has been investigated. In this case, it has been shown that the Bound of the family can experiment an increment of more than 100% when the emission time in similar to the coherence time. Only values of the coherence time above 4 emission times assure a Bound similar to that measured in absence of turbulence.

ACKNOWLEDGMENT

This work has been possible thanks to the Madrid Community (project MEFASRET: CCG06-UAH/DPI0748), to the Spanish Ministry of Science and Technology (project RESELAI: TIN2006-14986-CO2-01) and the Spanish Ministry of Public Works (project VIATOR: 70025-T05).

REFERENCES

[1] D. Langer and C. Thorpe, "Sonar based outdoor vehicle navigation andcollision avoidance," in *Proc. IEEE/RSJ International Conference on Intelligent Robots and Systems*, July 1992, pp. 1445–1450.

[2] S. Maeyama, A. Ohya, and S. Yuta, "Positioning by tree detection sensor and dead reckoning for outdoor navigation of a mobile robot," in *Proc. of the IEEE Conference on Multisensor Fusion and Integration for Intelligent Systems (MFI'94),* October 1994, pp. 653–660.

[3] M. E. Delany, "Sound propagation in the atmosphere: A historical review," *Acustica*, vol. 38, pp. 201–223, 1977.

[4] T. F. Embleton, "Tutorial on sound propagation outdoors," *Journal of the Acoustical Society of America*, vol. 100, no. 1, pp. 31–48, 1996.

[5] H. Peremans, K. Audenaert, and J. V. Campenhout, "A high resolution sensor based on tri-aural perception," *IEEE Transactions on Robotics and Automation*, vol. 9, pp. 36–48, February 1993.

[6] K.-W. J¨org and M. Berg, "Sophisticated mobile robot sonar sensing with pseudo-random codes," *Robotics and Autonomous Systems*, vol. 25, pp. 241–251, 1998.

[7] J. Ureña, M. Mazo, J. J. García, A. Hernández, and E. Bueno, "Classification of reflectors with an ultrasonic sensor for mobile robots applications," *Robotics and Autonomous Systems*, vol. 29, pp. 269–279, 1999.

[8] G. A. Daigle, J. E. Piercy, and T. F. W. Embleton, "Line-of-sight propagation through atmospheric turbulence near the ground," *Journal of the Acoustical Society of America*, vol. 74, pp. 1505–1513, 1983.

[9] F. J. Álvarez, J. Ureña, M. Mazo, A. Hernández, J. J. García, and C. Marziani, "High reliability outdoor sonar prototype based on efficient signal coding", *IEEE Trans. on Ultrasonics, Ferroelectrics and Frequency Control,* vol. 53, no. 10, pp. 1862–1871, October 2006.

[10] C. C. Tseng and C. L. Liu, "Complementary sets of sequences", *IEEE Transactions on Information Theory*, vol. IT-18, no. 5, pp. 644-652, September 1972.

[11] G. I. Taylor, "The spectrum of turbulence", in Proc. Of the Royal Society of London, Series A, vol. 164, pp. 476-490, February 1938.

[12] Polaroid Corp., "600 Series. Instrument Grade Electrostatic Transducers", Technical Specification, 1999